geodiversitas

2018 • 40 • 5

Camelus thomasi Pomel, 1893 from the Pleistocene type-locality Tighennif (Algeria). Comparisons with modern *Camelus*

Pietro MARTINI & Denis GERAADS

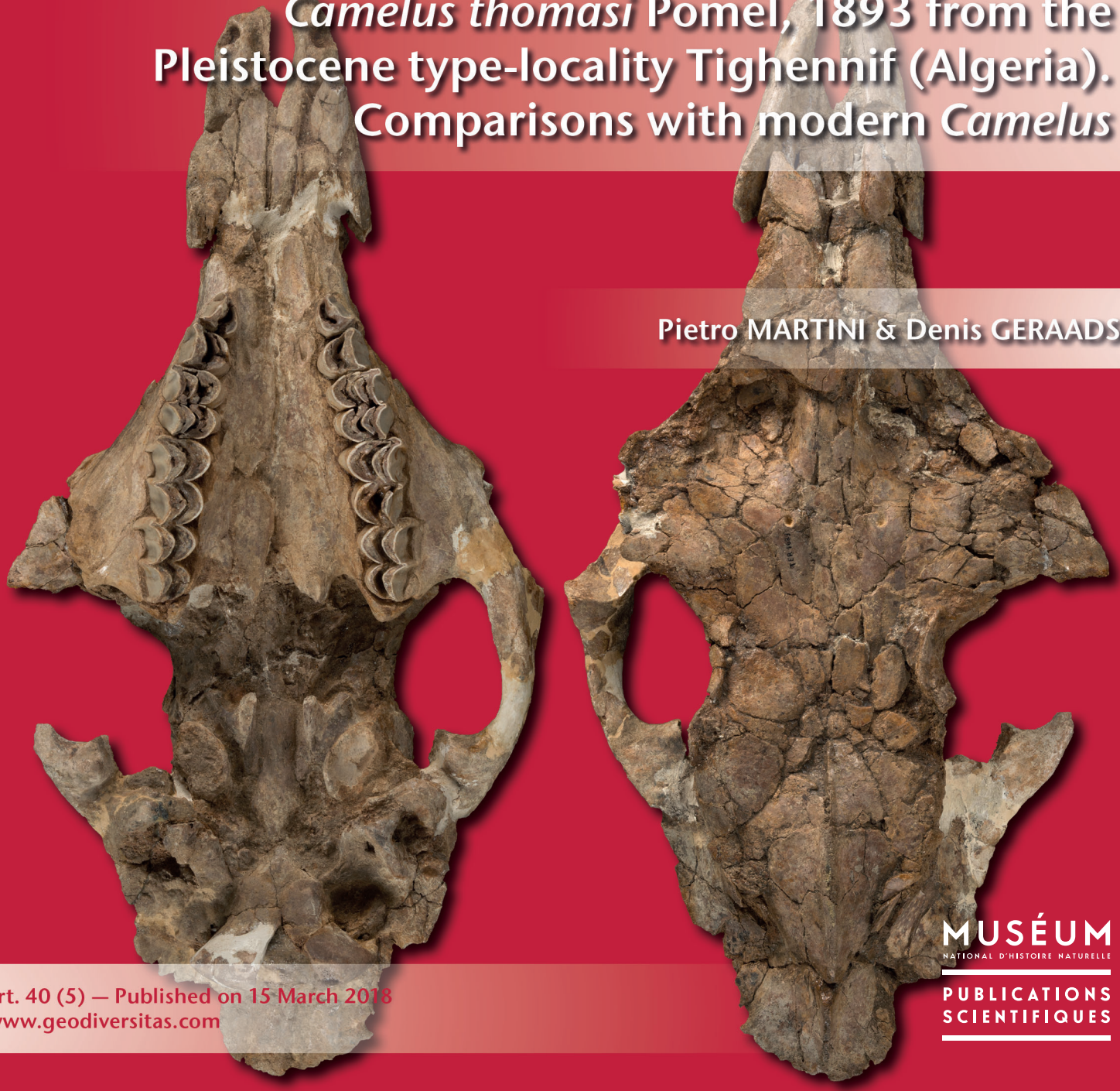

art. 40 (5) — Published on 15 March 2018
www.geodiversitas.com

MUSÉUM
NATIONAL D'HISTOIRE NATURELLE
PUBLICATIONS SCIENTIFIQUES

Geodiversitas est indexé dans / Geodiversitas *is indexed in:*
– Science Citation Index Expanded (SciSearch®)
– ISI Alerting Services®
– Current Contents® / Physical, Chemical, and Earth Sciences®
– Scopus®

Geodiversitas est distribué en version électronique par / Geodiversitas *is distributed electronically by:*
– BioOne® (http://www.bioone.org)

Les articles ainsi que les nouveautés nomenclaturales publiés dans *Geodiversitas* sont référencés par / *Articles and nomenclatural novelties published in* Geodiversitas *are referenced by:*
– ZooBank® (http://zoobank.org)

Geodiversitas est une revue en flux continu publiée par les Publications scientifiques du Muséum, Paris
Geodiversitas *is a fast track journal published by the Museum Science Press, Paris*

Les Publications scientifiques du Muséum publient aussi / *The Museum Science Press also publish:*
Adansonia, ***Zoosystema***, ***Anthropozoologica***, ***European Journal of Taxonomy***, ***Naturae.***

Diffusion – Publications scientifiques Muséum national d'Histoire naturelle
CP 41 – 57 rue Cuvier F-75231 Paris cedex 05 (France)
Tél. : 33 (0)1 40 79 48 05 / Fax : 33 (0)1 40 79 38 40
diff.pub@mnhn.fr / http://sciencepress.mnhn.fr

ISSN (imprimé / *print*) : 1280-9659/ ISSN (électronique / *electronic*) : 1638-9395

Camelus thomasi Pomel, 1893 from the Pleistocene type-locality Tighennif (Algeria). Comparisons with modern *Camelus*

Pietro MARTINI
Institut für Prähistorische und Naturwissenschaftliche Archäologie, Universität Basel,
Spalenring 145, 4055 Basel (Switzerland)
and Naturhistorisches Museum Basel, Augustinergasse 2, 4001 Basel (Switzerland)
pietro.martini@unibas.ch (corresponding author)

Denis GERAADS
Muséum national d'Histoire naturelle,
Centre de Recherche sur la Paléobiodiversité et les Paléoenvironnements (UMR 7207),
Sorbonne Universités, MNHN, CNRS, UPMC,
case postale 38, 57 rue Cuvier, F-75231 Paris cedex 05 (France)
and Max Planck Institute for Evolutionary Anthropology, Department of Human Evolution,
Deutscher Platz 6, D-04103 Leipzig (Germany)

Submitted on 12 May 2017 | accepted on 6 October 2017 | published on 15 March 2018

urn:lsid:zoobank.org:pub:75E0B79C-04FC-412D-ABC9-AB60B4B4E145

Martini P. & Geraads D. 2018. — *Camelus thomasi* Pomel, 1893, from the Pleistocene type-locality Tighennif (Algeria). Comparisons with modern *Camelus*. *Geodiversitas* 40 (5): 115-134. https://doi.org/10.5252/geodiversitas2018v40a5. http://geodiversitas.com/40/5

ABSTRACT
We describe here the whole collection of *Camelus thomasi* Pomel, 1893 from the Pleistocene type-locality Tighennif (Ternifine) in Algeria. Detailed morphological and metric comparisons with the two species of modern *Camelus* Linnaeus, 1758, *C. bactrianus* Linnaeus, 1758 and *C. dromedarius* Linnaeus, 1758, show that it is clearly distinct from both of them. It is mainly characterized by pachyostosis especially marked in the mandible, a size slightly greater than modern forms, broad molars with strong styles, and several unique cranial features. The species seems restricted to the terminal Early Pleistocene and is not definitely known outside Northwestern Africa. A phylogenetic analysis is premature, but *C. thomasi* does not appear to be particularly close to either modern species, and there is no support to regard it as an ancestor of the dromedary.

KEY WORDS
Mammalia,
Camelidae,
Pleistocene,
Algeria,
morphometrics.

RÉSUMÉ
Camelus thomasi *Pomel, 1893 du Pléistocène de la localité-type Tighennif (Algérie). Comparaisons avec les* Camelus *actuels.*
Nous décrivons ici l'ensemble de la collection de *Camelus thomasi* Pomel, 1893 de la localité-type, Tighennif (Ternifine) en Algérie. Des comparaisons morphologiques et métriques détaillées avec les deux *Camelus* Linnaeus, 1758 actuels, *C. bactrianus* Linnaeus, 1758 and *C. dromedarius* Linnaeus, 1758, montrent que la forme fossile est clairement distincte de l'une comme de l'autre. Elle est principalement caractérisée par une pachyostose spécialement marquée sur la mandibule, une taille un peu supérieure, des molaires larges avec de forts styles, et plusieurs traits crâniens uniques. L'espèce semble restreinte au Pléistocène inférieur terminal, et n'est pas attestée en dehors du Maghreb. Une analyse phylogénétique serait prématurée, mais *C. thomasi* ne semble pas spécialement proche de l'une ou l'autre des formes modernes, et rien ne permet de la considérer comme l'ancêtre du dromadaire.

MOTS CLÉS
Mammalia,
Camelidae,
Pléistocène,
Algérie,
morphométrie.

TABLE 1. — List of specimens of *Camelus thomasi* Pomel, 1893 described in this study.

Specimen	Side	Element	Preservation
OH1-GDR F14-87	–	maxilla	fragment, with M1-M2
MNHN.F.TER1647	sin	metacarpale	proximal fragment
MNHN.F.TER1648	dex	metacarpale	complete
MNHN.F.TER1649	sin	tibia	distal fragment
MNHN.F.TER1650	dex	tibia	distal fragment
MNHN.F.TER1651	dex	metatarsale	distal fragment
MNHN.F.TER1652	–	metacarpale	diaphysis and left condyle
MNHN.F.TER1653	–	metacarpale	distal fragment
MNHN.F.TER1654	–	metacarpale	distal fragment
MNHN.F.TER1655	sin	metatarsale	proximal fragment
MNHN.F.TER1656	dex	metatarsale	proximal fragment
MNHN.F.TER1657	dex	metatarsale	proximal fragment
MNHN.F.TER1658	dex	metatarsale	proximal fragment
MNHN.F.TER1659	–	metacarpale	distal condyle
MNHN.F.TER1660	sin	fibula	lateral malleolus
MNHN.F.TER1661	–	metacarpale	proximal fragment
MNHN.F.TER1662	dex	metatarsale	proximal fragment with diaphysis
MNHN.F.TER1663	sin	metatarsale	proximal fragment with diaphysis
MNHN.F.TER1664	dex	metatarsale	complete
MNHN.F.TER1665	dex	calcaneus	–
MNHN.F.TER1666	sin	calcaneus	–
MNHN.F.TER1667	dex	calcaneus	–
MNHN.F.TER1668	sin	calcaneus	–
MNHN.F.TER1669	dex	astragalus	–
MNHN.F.TER1670	dex	astragalus	–
MNHN.F.TER1671	sin	astragalus	–
MNHN.F.TER1672	dex	astragalus	–
MNHN.F.TER1673	–	phalanx proximal posterior	complete
MNHN.F.TER1674	–	phalanx proximal anterior	complete
MNHN.F.TER1675	–	phalanx proximal anterior	complete
MNHN.F.TER1676	–	phalanx proximal anterior	complete
MNHN.F.TER1677	–	phalanx proximal anterior	complete
MNHN.F.TER1678	dex	naviculare	–
MNHN.F.TER1679	dex	naviculare	–
MNHN.F.TER1680	dex	ectomesocuneiforme	–
MNHN.F.TER1681	sin	metacarpale	complete but missing distal condyles
MNHN.F.TER1682	dex	tibia	complete with damaged distal cochlea
MNHN.F.TER1683	sin	hemimandibula	with complete ramus, m2-m3, and alveoles of p4-m1; likely the same individuals as TER1684
MNHN.F.TER1684	dex	hemimandibula	with damaged ramus, m2-m3, broken at the level of the alveoles of m1; likely the same individuals as TER1683
MNHN.F.TER1685	dex	hemimandibula	with complete ramus and p4-m3
MNHN.F.TER1686	dex	hemimandibula	fragment, with fragment of ramus and broken m3
MNHN.F.TER1687	sin	hemimandibula	fragment, with highly damaged m3
MNHN.F.TER1688	dex	hemimandibula	fragment, with highly damaged m2-m3

INTRODUCTION

In one of his important monographs dealing with fossil mammals from Algeria, Pomel (1893) described a new species of camel as *Camelus thomasii* [sic] Pomel, 1893, based upon a fragment of maxilla, a piece of mandible and an incomplete metatarsal, from the locality then called Palikao, but better known in the literature as Ternifine (now Tighennif; Geraads [2016], and references therein). He noted that the type maxilla differs from that of the modern dromedary in the shape of the maxillo-palatine suture and in the horizontal orbital floor, supposedly giving the animal a less stupid look (‘*un air moins stupide*’) than the dromedary, in which the orbits face more downwards. Further excavations at the site, mostly by C. Arambourg in 1954-1956 (Arambourg & Hoffstetter 1963; Geraads *et al.* 1986), much increased the camel collection, which is now by far the richest sample of African fossil camels. However, in spite of its importance, this collection remained unstudied, besides short descriptions by Harris *et al.* (2010). That explains why the species has been erroneously reported from a number of other sites and, most regrettably, its systematic position discussed without reference to the material from the type-locality. Here we describe the whole collection of *C. thomasi* from Tighennif, and discuss its relationships with the extant dromedary *C. dromedarius* Linnaeus, 1758 and Bactrian camel *C. bactrianus* Linnaeus, 1758.

MATERIALS AND METHODS

Most of the material of *C. thomasi* described below (Table 1) is housed in the Collection of Palaeontology of the Muséum national d’Histoire naturelle, Paris (MNHN.F); in addition, we have seen photos of the specimens (including the type) kept in the Algiers Museum, kindly provided by Y. Chaïd-Saoudi. A few other potential specimens of *C. thomasi* are

FIG. 1. — *Camelus thomasi* Pomel, 1893, Tighennif (Algeria), cranium, MNHN.F.TER1689: **A**, left lateral view; **B**, ventral view of the cranial basis (stereo); **C**, ventral view; **D**, dorsal view. Scale bar: 40 cm.

from the 'Grotte des Rhinocéros' in Casablanca (Geraads & Bernoussi 2017). We have compared them to a good sample of modern camels: *C. bactrianus* (28 skulls), *C. dromedarius* (31 skulls), hybrids or unidentified (3 skulls), housed in MNHN, CCEC, ZIN, ZM, NMBE, NMB, MHNG, MSNM, and EK using the measurements of Martini *et al.* (2017). We have not attempted to distinguish taxonomically wild, feral and domestic forms of *C. bactrianus*, because such information is almost always missing in osteological collections.

Abbreviations

CCEC	Centre de Conservation et d'Études des Collections, Lyon;
EK	Tell Arida research centrum, El Kowm, Syria;
INSAP	Institut national des Sciences de l'Archéologie et du Patrimoine, Rabat;
IPH	Institut de Paléontologie humaine, Paris;
MGA	Musée de Géologie, Algiers;
MHNG	Muséum d'Histoire naturelle de la Ville de Genève;
MNHN	Muséum national d'Histoire naturelle, Paris;
MSNM	Museo Civico di Storia Naturale, Milano;
NMB	Naturhistorisches Museum, Basel;
NMBE	Naturhistorisches Museum des Burgergemeindes Bern;
ZIN	Zoological Institute, Russian Academy of Sciences, Saint Petersburg;
ZM	Zoologisches Museum der Universität Zürich.

SYSTEMATIC PALAEONTOLOGY

Family Camelidae Gray, 1821

Genus *Camelus* Linnaeus, 1758

Type species. — *Camelus bactrianus* Linnaeus, 1758 by original designation.

Camelus thomasi Pomel, 1893

Camelus thomasi Pomel, 1893: 14.

Camelus thomasii – Pomel 1886: 504 (*nomen nudum*).

Holotype (by original designation). — Right maxilla with M1-M2 and part of the palatine bone, no. 7236001 in the *Musée de Géologie*, Algiers, Algeria (Fig. 2E); also Pomel (1893: pl. 3, figs 2-5; note that Pomel's figures are inverted, and that the association of a M3 with this maxilla is tentative). From the late/terminal Early Pleistocene of Tighennif (formerly spelled "Tighenif", also known as Ternifine or Palikao), near Mascara, Algeria.

Referred material. — The whole collection of *Camelus* from Tighennif is referred to this species; the full list of specimens housed in MNHN and their measurements are given in the Table 1. In addition, we tentatively ascribe to the same species some specimens from the Middle Pleistocene of Oulad Hamida I quarry in Morocco, but they do not contribute to the definition of the species.

Diagnosis. — A *Camelus* slightly larger than the modern species; pachyostosis weakly indicated in cranium (thick nasalia, thickening of the zygomatic arch posteriorly) and strongly so in the mandible; marked sexual dimorphism; V-shaped choanae; palatine foramina located anteriorly, at the level of P3 or P4; facial crest present; low placement of orbits; paroccipital process far from condyles; teeth small relatively to skull size; P1 located anteriorly, P3 with a complete lingual crescent; molars alveolarly broad with strong styles; mandible thick and low, especially anteriorly; coronoid process short, massive, slightly twisted and bent backwards; caudal mental foramen located anteriorly, or absent; p1 absent or located more anteriorly than in modern forms; p4 long, with a long metaconid; limb bones long; tibial tuberosity slender and very prominent; phalanges robust.

Age of the site. — Historical data on the excavations and research at Tighennif can be found in Geraads (2016), who provided a faunal list, and concluded that the site is probably older than the Middle Pleistocene, as also assumed by Sahnouni & van der Made (2009); it can tentatively be dated to *c.* 1 Ma. It is best known for its hominin remains (Arambourg & Hoffstetter 1963), either referable to *Homo rhodesiensis* Woodward, 1921 (according to Hublin 2001) or closer to *H. ergaster* (Martinón-Torres *et al.* 2007).

Description and comparisons with modern forms

The best specimen is a relatively complete cranium, MNHN.F.TER1689 (Fig. 1), first figured by Lhote (1987). Its description can be complemented with that of other cranial elements: the maxilla with imperfectly preserved teeth TER1816 (Fig. 2A), and the type-specimen MGA-7236001 (on the basis of photos kindly provided by Y. Chaïd-Saoudi, Fig. 2B). Unfortunately, TER1689 is strongly dorso-ventrally crushed, so that the cranial surface consists of a mosaic of bone fragments among which sutures and details are hard to recognize. This crushing prevents reconstruction of the dorsal cranial profile and of the position of the front teeth relative to the occlusal plane of the cheek teeth. The basicranium is also poorly preserved and the right zygomatic arch is missing. In addition, the premaxillae are somewhat shifted posteriorly, and probably lack a few mm at their tips. By contrast, the moderately worn cheek-teeth are nicely preserved, but all teeth anterior to P3 are missing, except the left canine.

Overall size is close to the maximum seen in extant species (Appendices 1-3). The maximal length (measurement C1) of 575 mm exceeds that of all 31 measured *C. dromedarius*, and was surpassed (by less than 10 mm) in only two individuals out of 28 *C. bactrianus*; given that this measurement is certainly underestimated because of the preservation of the premaxillae, it can reasonably be assumed that this skull was longer than that of all modern *Camelus* in our sample. Beside the larger size, the only proportions that differ significantly from those of the modern forms are the ones that indicate a shorter face and rostrum; considering the imperfect preservation of the premaxilla, these differences can probably be ignored. Dorso-ventral crushing prevents fully reliable estimates of breadth at orbital and post-orbital levels, but on the whole there is no evidence that general cranial proportions differed much from modern forms.

Rostrum

The premaxillae taper anteriorly, so that the rostrum appears pointed but it is certainly partly eroded; in both modern forms, its shape is variable, from similar to that of MNHN.F.TER1689 to distinctly broadened. The nasal opening looks small, but this is probably an impression given by the medial folding of the maxilla and misplacement of the premaxilla. Because of this crushing, the topographic relationships of the premaxillae

Fig. 2. — *Camelus thomasi* Pomel, 1893, Tighennif (Algeria): **A**, maxilla MNHN.F.TER1816, occlusal view; **B**, maxilla with M1-M2 and tentatively associated M3, holotype no. 7236001; **B1**, right lateral view; **B2**, occlusal view; **C**, partial mandible 1900-27, dorsal view; **D**, partial mandible TER1688, dorsal view; **E**, partial mandible TER1686, dorsal view; **F**, mandible TER1683; **F1**, dorsal view; **F2**, lateral view; **G**, mandible TER1685; **G1**, dorsal view; **G2**, medial view. Holotype no. 7236001 (**B**) is housed in the *Musée de Géologie* (Algier); all others specimens are housed in the MNHN. Scale bar: F2, G2, 40 cm; 20 cm for all others.

cannot be definitely ascertained. Their most remarkable feature is their thickness throughout their length, which contrasts with their slenderness in the modern forms.

The infra-orbital foramen is located above the limit between P4 and M1; it occupies the same position in the maxilla MNHN.F.TER1816, and usually also in extant forms.

The front border of the orbit is located above the posterior half of M2, thus much like in modern forms, in which it is almost always located above that tooth as well. The orbit itself is too crushed for its real shape and measurements to be estimated, but it was located rather close to the tooth-row (Fig. 3). A long facial crest runs more or less parallel to its

ventral border, about 25 mm below it; it fades out anteriorly and posteriorly, without connecting the ventrolateral edge of the zygomatic arch; the maxilla MNHN.F.TER1816 is imperfectly preserved below the orbit, but the facial crest was probably absent. It is almost always wholly absent in *C. dromedarius* (CCEC 5000-2069 being the single exception), but it is at least incipient in *C. bactrianus*, although it usually talks the shape of a tubercle below the anterior orbital border. Another crest underlines the ventral orbital border, about 10 mm below it, and proceeds posteriorly into the ventro-lateral edge of the zygomatic arch, as in modern *Camelus*. The front end of the squamosal is located about 25 mm behind the orbit. As mentioned above, the shape of the nasals cannot be determined. The ethmoid fissure was at most very small, and probably absent; in *C. bactrianus* its size ranges from large to extremely small, in *C. dromedarius* from medium-sized to absent. Around their position, on either side of the posterior part of the nasals, the dorsal part of the skull bears two symmetrical depressions due to post-mortem crushing but whose formation was certainly facilitated by the thinness of bones in this area, and underlying sinuses. The supra-orbital foramina are located not far apart (46 mm), as in modern forms, where they are often multiple.

Braincase

The sagittal crest suffered no major distortion; it starts behind the post-orbital constriction but remains low and, even in its caudal portion, never becomes blade-like as often occurs in male *C. dromedarius*. As it now stands, the nuchal crest is thin and convex in occipital view, but it is probably incompletely preserved. In the sagittal plane, the occipital crest is stronger than in most recent *Camelus*. There was certainly no large nuchal tubercle above the foramen magnum, as sometimes occurs in *C. bactrianus*.

Palate

The ventral view confirms the tapering rostrum and short, pointed premaxillae. The large canine identifies the skull as that of a male. The P1 is missing, and its alveolus cannot be identified, but the individual was probably too young for having shed this tooth, as happens in senile individuals of the modern form. However, if present, this tooth was certainly closer to the canine than to P3, a position closer to the state of *C. dromedarius*, whereas in *C. bactrianus* this tooth is more posterior.

The palate is slightly crushed transversally, so that the outline of the choanae is imperfectly preserved; however, it was certainly much closer to the V shape that is most common in *C. bactrianus*, but is never found in *C. dromedarius*. MNHN.F.TER1816 almost certainly also had narrow V-shaped choanae. The choanae reach the level of the front of M3, which is not rare in *C. bactrianus*, but which we observed in a single, very old specimen of *C. dromedarius*. The course of the maxillo-palatine suture cannot be followed, as is normal in adult camels.

In MNHN.F.TER1689, the palatine foramina open at the level of P4, which is the most common position in *C. dromedarius*, whereas those of *C. bactrianus* almost always open at the level of M1 or M2. They are even more anterior in MNHN.F.TER1816, at the level of the posterior part of P3.

Basicranium

The pterygoid wings are missing, but the pterygoid processes of the basisphenoid consist of thick blades that emerge at the level of the middle of the glenoid fossae; in modern *Camelus*, they remain instead fully anterior to these fossae. The processes lateral to the foramen orbitorotundum are robust.

The glenoid fossae are incompletely preserved; they are deeply concave and bordered laterally by a thick, but low tubercle that is less lateral than in modern forms, because some thickening of the posterior root of the zygomatic arch occurred, laterally to this tubercle.

The auditory region is too poorly preserved for description, but a sharp difference with both modern species is that the paroccipital processes are located much farther from the occipital condyles, from which they are separated by a long, deep fossa, which is much shorter in modern camels; consequently, the tips of the paroccipital processes are farther apart than in modern forms. The condyles are broad (Fig. 4) and markedly extend onto the basioccipital, as in most *C. bactrianus*, whereas they may be shorter antero-posteriorly in *C. dromedarius*, but the morphology of *C. thomasi* is within the variation of both modern species.

Dentition

In contrast to skull length, length M1–M3 of the complete skull (C34 = 114 mm), is close to the mean value for *C. bactrianus*, but it is even distinctly lower (102 mm) in MNHN.F.TER1816, close to the mean of *C. dromedarius*. The cheek-teeth are little worn and very well preserved. Although no tooth is quite fresh, the slight wear of the premolars, and of the M3 tentatively associated with the type-maxilla, show that the degree of hypsodonty was very similar to that of modern *Camelus*. No cement cover is preserved on any tooth, in contrast to modern forms in which it is present; it was probably destroyed during fossilization, or removed during preparation, because it is present in some lower teeth, and because Pomel (1893: pl. 4, fig. 1) figured cement on an upper molar from Tighennif. The P3 has a complete lingual wall; the central valley is fully closed lingually, and opens mesially 13 mm above the cervix. The lingual crescent is never complete in *C. dromedarius*, and very rarely complete in *C. bactrianus*; in these forms, P3 is usually a reduced tooth, quite different from P4, whereas they are similar in *C. thomasi*. Thus, although this tooth is present only in MNHN.F.TER1689, the difference with modern forms is clear. P4 differs from P3 only in being larger and more symmetrical; on both teeth the buccal central rib is quite weak, and the mesial and distal styles are buccally prominent. M1 has a small basal cingulum along the lingual side; this tooth is distinctly smaller than M2, which is about as large as M3. On all molars, the buccal paracone rib is better indicated than the vestigial metacone rib, the parastyle is thicker than the mesostyle but both are quite prominent bucally, in contrast to the metastyle, which is distinct on M3

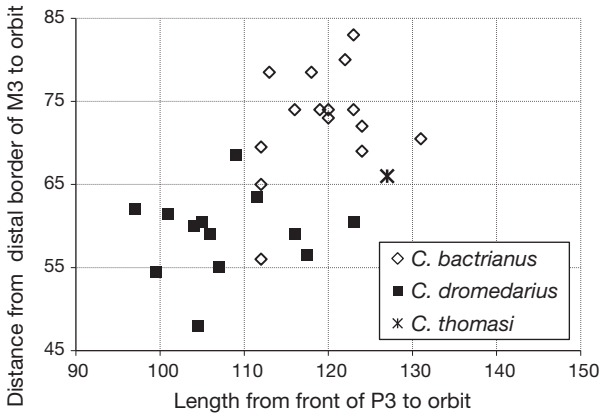

Fig. 3. — Bivariate plot of cranial measurements of *Camelus bactrianus* Linnaeus, 1758, *C. dromedarius* Linnaeus, 1758 and *C. thomasi* Pomel, 1893 showing the position of the orbit (C24 vs C14 of Martini *et al.* 2017).

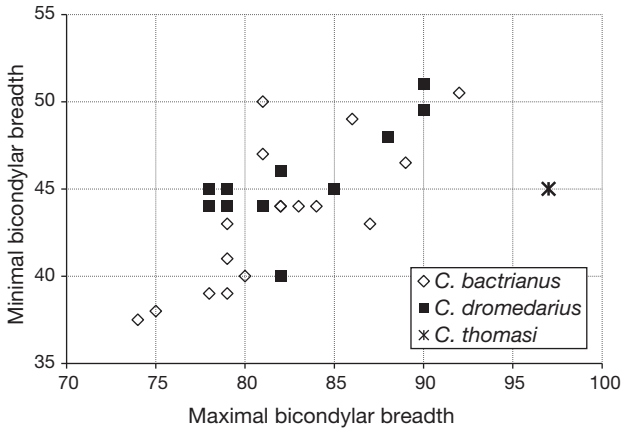

Fig. 4. — Bivariate plot of measurements of occipital condyles of *Camelus bactrianus* Linnaeus, 1758, *C. dromedarius* Linnaeus, 1758 and *C. thomasi* Pomel, 1893 (C74 vs C73 of Martini *et al.* 2017).

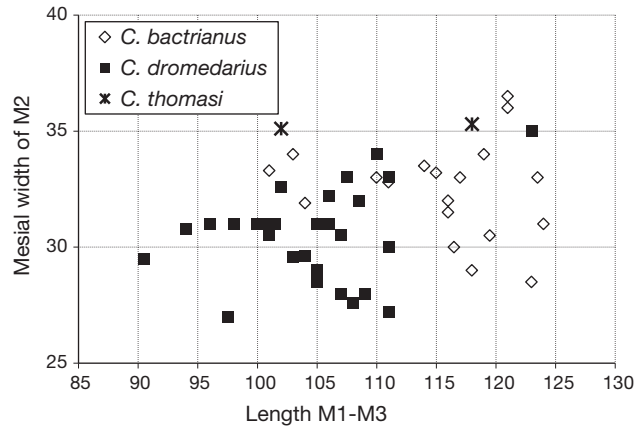

Fig. 5. — Bivariate plot of M2 mesial width vs length of molar row of *Camelus bactrianus* Linnaeus, 1758, *C. dromedarius* Linnaeus, 1758 and *C. thomasi* Pomel, 1893 (C34 vs Ds24 of Martini *et al.* 2017).

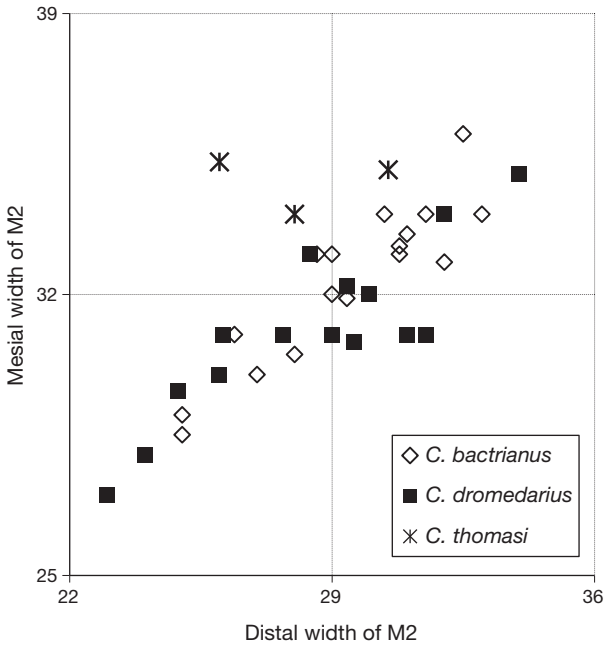

Fig. 6. — Bivariate plot of mesial vs distal widths of M2 of *Camelus bactrianus* Linnaeus, 1758, *C. dromedarius* Linnaeus, 1758 and *C. thomasi* Pomel, 1893 (Ds24 vs Ds25 of Martini *et al.* 2017).

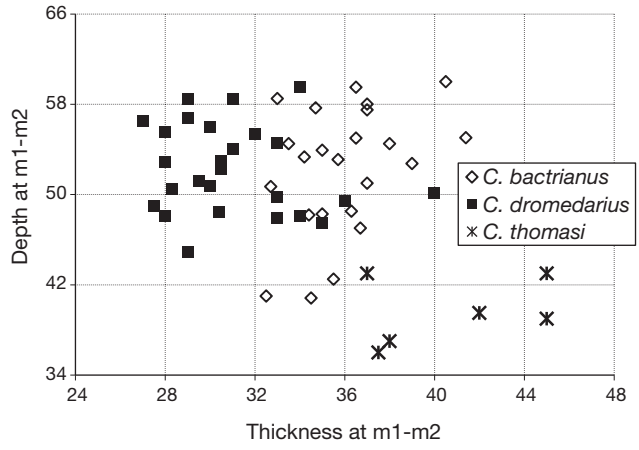

Fig. 7. — Bivariate plot of depth vs thickness of the mandibular corpus of *Camelus bactrianus* Linnaeus, 1758, *C. dromedarius* Linnaeus, 1758 and *C. thomasi* Pomel, 1893 (M20 vs M15 of Martini *et al.* 2017).

only. All these dental features are similar on the other specimens MNHN.F.TER1816 and MGA-7236001. In modern forms, the styles are less prominent buccally, especially the parastyle, which is not stronger than the mesostyle; there is variation in this regard, but the fact that both the type and TER1816 also have prominent styles suggest that this is a valid difference.

In addition, the molars differ from those of modern forms in being broader, in particular the mesial lobe of M1 and M2 (Figs 5, 6); although these can be accurately measured only in MNHN.F.TER1689, this was clearly also true in the smaller maxilla TER1816 (Fig. 1H).

Pomel (1893: pl. 4, figs 3, 4) tentatively ascribed to *C. thomasi* a mandible not found *in situ*, and now preserved in MGA; it fails to show the typical characters of the species, described below, and is probably of a historical *C. dromedarius* instead. The MNHN collection of *C. thomasi* from Tighennif includes seven partial mandibles, of which five are illustrated here:

Fig. 8. — *Camelus thomasi* Pomel, 1893, Tighennif (Algeria): **A**, metapodials, from left to right metatarsals MNHN.F.TER1664, TER1690, and metacarpals TER1648, TER1681, and TER1652; **B**, right tibia TER1682; **B1**, lateral view; **B2**, proximal view; **C**, left astragalus TER1670; **C1**, anterior view; **C2**, plantar view; **C3**, medial view; **C4**, distal view; **D**, left calcaneus TER1666; **D1**, anterior view; **D2**, plantar view; **D3**, medial view; **E**, left cuboid 1982-5-60; **E1**, proximal view; **E2**, distal view; **E3**, medial view; **F**, right navicular TER1679; **F1**, proximal view; **F2**, distal view; **F3**, lateral view. Scale bar: A, B, 40 cm; 20 cm for all others.

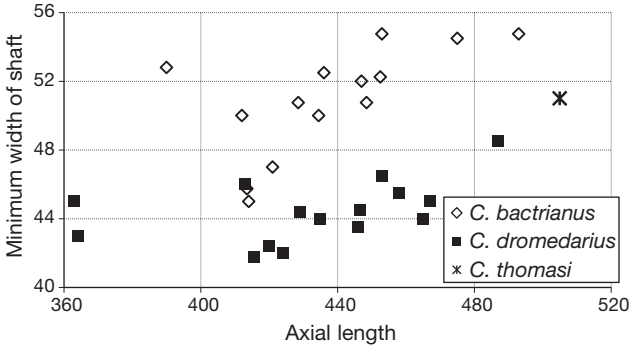

FIG. 9. — Bivariate plot of width of shaft vs length of the tibia of *Camelus bactrianus* Linnaeus, 1758, *C. dromedarius* Linnaeus, 1758 and *C. thomasi* Pomel, 1893 (Ti13 vs Ti3 of Martini *et al.* 2017).

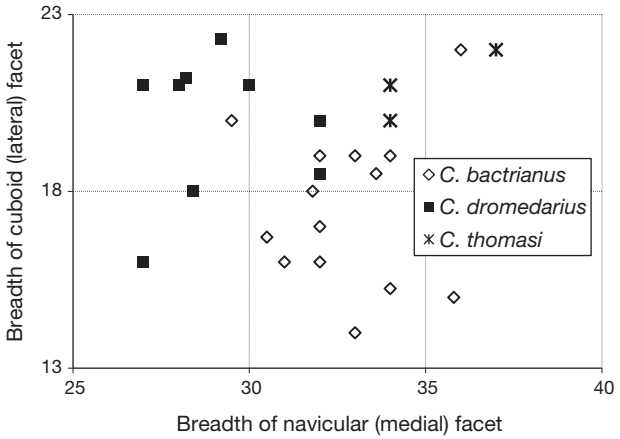

FIG. 10. — Bivariate plot of the widths of the cuboid facet vs navicular facet of the astragalus of *Camelus bactrianus* Linnaeus, 1758, *C. dromedarius* Linnaeus, 1758 and *C. thomasi* Pomel, 1893 (Ta15 vs Ta14 of Martini *et al.* 2017).

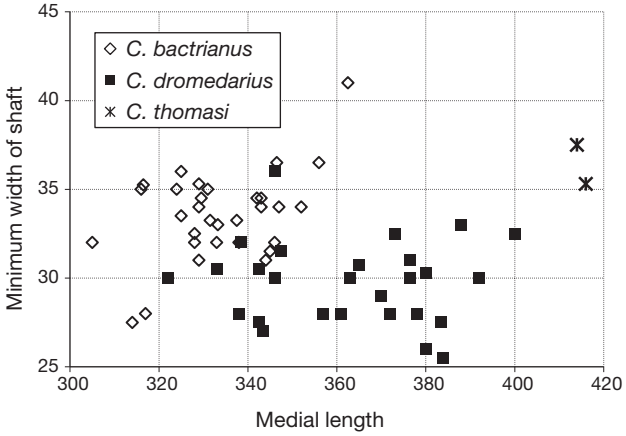

FIG. 11. — Bivariate plot of width of shaft vs length of the metatarsus of *Camelus bactrianus* Linnaeus, 1758, *C. dromedarius* Linnaeus, 1758 and *C. thomasi* Pomel, 1893 (Mp12 vs Mp1 of Martini *et al.* 2017).

MNHN.F.TER1683 (Fig. 2F; almost certainly of the same individual as TER1684); TER1685 (Fig. 2G); TER1900-27, collected by Pallary (Fig. 2C); TER1686 (Fig. 2E); and TER1688 (Fig. 2D). Two additional mandibles are stored in IPH and MGA.

Their most obvious character is the strong pachyostosis, the corpus being low but extremely thick below the cheek-teeth, and even thicker than deep below p4-m1 (Fig. 7); this thickening extends to the ascending ramus. The coronoid process is rather cylindrical with a flattened anterior surface, not blade-like. It is slanted backwards, with a weak curvature; its apex is transversally compressed, antero-posteriorly deeper than the base and has a slight lateral twist. This morphology contrasts with both species of modern *Camelus*, which are also different from each other. The condyle is preserved on MNHN.F.TER1685; it is rectangular, and antero-posteriorly short. This contributes, in addition to the shape of the coronoid process and reduction of the sigmoid notch, to the antero-posterior narrowness of the ramus at this level, in the three specimens in which this part is preserved.

MNHN.F.TER1683 (Fig. 2F) preserves a large part of the corpus anterior to p4, up to about 1 cm in front of the anterior mental foramen, and there is no evidence of a p1, so that this tooth was either absent, or more anterior. In modern *Camelus*, p1 is almost always present, and can be shed only in individuals distinctly older than TER1683; it is never as anterior as it must have been if present in TER1683.

The posterior mental foramen is located below the anterior part of m1 in MNHN.F.TER1685, but is certainly absent in TER1683/TER1684. It is not visible in the other specimens, which preserve only the posterior part of the mandible, but if present it was always anterior to the middle of m1, a position more similar to that observed in *C. bactrianus*, whereas it is more posterior in *C. dromedarius*.

The only preserved p4 is that of MNHN.F.TER1685. It is longer than that of modern form; the metaconid is antero-posteriorly expanded to form a complete lingual wall; this sometimes occurs in *C. bactrianus*, but never in *C. dromedarius*.

In all camel species, the upper part of the lingual wall of the lower molars is concave between the stylids, but as wear proceeds, the styles fade away, and the lingual walls become more or less flat; they may even become slightly convex, perhaps especially so in *C. thomasi*. There is some variation in the shape of the third lobe of m3, but its lingual wall is less oblique than the average condition of modern forms.

There are a number of post-cranial bones in the Tighennif sample but preservation of most of them is imperfect, and precise measurements can seldom be taken (Tables 3, 4). Still, it is clear that they are larger than those of living *Camelus*; in particular, all long bones whose length can be measured or reasonably estimated are longer than the modern maxima.

The scapula, humerus, radio-ulna, and carpals are not represented. There are some, mostly incomplete metacarpals (Fig. 8A); those of the Bactrian camel differ from those of the dromedary in being shorter and stouter; those of *C. thomasi* are significantly longer than all of them, but the diaphyses are relatively as robust as in *C. bactrianus*. In contrast, the distal articulation is narrow. MNHN.F.TER1652 is aberrant in its wide distal condyle, but the morphology of this part suggests plastic distortion. Other individuals show condyles which are deeper than wide, closer in this respect to dromedaries.

There is no femur, but there is an almost complete tibia MNHN.F.TER1682 (Fig. 8B) and two incomplete distal

epiphyses. This bone is also longer than all modern ones, and distinctly more gracile than those of the Bactrian camel (Fig. 9). The proximal epiphysis differs clearly from both modern species in the narrow, transversely compressed but antero-posteriorly expanded anterior tuberosity (Fig. 8B2); it is much thicker and much less prominent in modern forms.

The single fibula is large and it is in particular wide. Although the distal tibiae are poorly preserved, the lateral facet of the distal cochlea appears to agree with the proportions of the fibula.

The calcanei (Fig. 8D) are large and overall similar to *C. bactrianus*, particularly in their shorter and less constricted tuber and the anterior placement of the sustentaculum; but the fibular trochlea is smaller and less prominent, and the plantar border is broad (except in MNHN.F.TER1665 that may not be fully adult), more like in the dromedary.

There are four astragali, of which only one is well-preserved (Fig. 8C). The proximo-lateral lip ranges from short as in *C. bactrianus*, to long as in *C. dromedarius* (Steiger 1990). Distally, the facet for the navicular (the lateral part of the trochlea) is relatively small (Fig. 10), more similar to *C. bactrianus* than to *C. dromedarius* (in which this facet is more similar in width to the facet for the cuboid).

A single cuboid (Fig. 8E), collected in 1982 (Geraads *et al.* 1986) is large and high; the astragalar facet is narrow, as in *C. bactrianus*. On the lateral side, the groove for the tendon of the m. peroneus longus is shallower than in modern forms.

The navicular (Fig. 8F) is represented by two specimens that are low and wide, with proportions rather similar to *C. bactrianus*. Other known small bones include the trapezoideum and the intermedio-lateral cuneiform, which are similar to extant species.

The two metatarsals whose length can be estimated are, like the metacarpals, much longer than in modern *Camelus* (Fig. 11). The proximal epiphysis is relatively small. The facet for the cuboid is transversally wide, while the facet for the medial cuneiform is shortened. The distal articulation of the metatarsal is narrower than in *C. bactrianus*.

There are four anterior and one posterior phalanges. They are longer than in modern forms, and more massive, being less constricted at mid-length. The condyles appear narrow and seem to have less asymmetric lips than in extant species, where the abaxial lip is longer.

DISCUSSION

The first issue regarding the Tighennif camel sample is that of its species homogeneity. Although size variation of the post-cranial remains can be accommodated within a single species, there are important size differences between, e.g., skull MNHN.F.TER1689 and maxilla TER1816, or between the mandibles TER1683/TER1684 and all other mandibles. However, all mandibles share the same remarkable pachyostosis and related features, and both TER1689 and TER1816 share strong styles, broad molars, and anteriorly located palatine foramina. We therefore conclude that the whole collection belongs to a single species, whose important size variation can be explained by sexual dimorphism.

The most remarkable feature of *C. thomasi* is its pachyostosis, which strongly affects the mandible, moderately the skull, but not the postcranials. This tissue distribution is similar to what is found in several megacerine Cervidae (see references in Morales *et al.* 1993), in which the mandible is also the most affected part, but not to what occurs in the lower Miocene *Lorancameryx* Morales, Pickford & Soria, 1993 from Spain (Morales *et al.* 1993), in which it is the anterior limb that underwent the most spectacular pachyostosis. Besides some aquatic forms, in which it is obviously related to the need for increasing density, pachyostosis (defined as deposition of extra bone, by comparison with closely related forms) is rare in mammals and restricted, as far as we know, to a few Cetartiodactyla and *Homo* of the *erectus* group, so that general explanations are unlikely to be valid. The occurrence of pachyostosis in Cervidae, in which large amounts of bone are deposited every year, might be explained as a side-effect of antler formation, but its origin in *C. thomasi* remains obscure. Clearly, the heavy mandible of all camels, compared with similar-sized selenodont Cetartiodactyla, provided a basis for this hyper-ossification. This pachyostosis might be dependent of environmental conditions and therefore it might be limited to the Tighennif population, but since this is the type locality we include this character in the diagnosis of this species

Some of the other morphological and metric features described above are closer to those of *C. dromedarius*, more of them are closer to *C. bactrianus*, but there are also some major features which unambiguously demonstrate that *C. thomasi* is distinct from both modern species, as listed in the diagnosis. Pending full study of recently collected material from Syria and Ethiopia, critical to the history of Old World Camelidae, a phylogenetic analysis would be premature, but now that *C. thomasi* is satisfactorily characterized, some conclusions regarding the distribution of the species can be drawn.

From the 'Grotte des Rhinocéros' near Casablanca, dated to *c.* 0.5 Ma, Geraads & Bernoussi (2017) reported some remains that they assigned to this species. Two upper molars OH1-GDR F14-87 do not have strong styles but are broader than in modern forms, as at Tighennif; a m3 E12-26 is broad as well. A virtually complete metacarpal GDR-5271 is about as long as the largest Tighennif bones, and remarkably robust, as several of its measurements even exceed the Tighennif ones. We can assume that these remains represent an advanced form of *C. thomasi*, which further increased the size and robustness of its bones, but positive identification cannot be reached without cranial or mandibular material.

Gautier (1966) reported *C. thomasi* from Northern Sudan, in a site dated to *c.* 22 000 BP. He estimated, on the basis of field photographs, that the length of some limb-bones was about 1.2-1.4 times longer than in modern forms (compared to one individual of each species). In fact, some

of the bones (distal tibia, calcaneum) indicate that this animal was significantly larger than *C. thomasi*. This large size is partly confirmed by a mandible (not figured) whose measurements are slightly above those of modern *Camelus*. Moreover, Gautier's identification was not supported by any morphological feature, and in particular there is no mention of mandibular pachyostosis. Unfortunately, this paper led the way to numerous mentions of *C. thomasi* in the African and Arabian Late Pleistocene to Holocene, giving the deceitful impression that this species was widespread and persisted until historic times. For instance, Grigson (1983) suggested that a very large camel from the late Pleistocene of Israel might represent *C. thomasi*; again, the measurements that she provided are much larger than those of this species (e.g., breadth of distal metapodial condyle = *c.* 58 mm, vs 36-52 mm at Tighennif; breadth of proximal metacarpal = *c.* 90 mm, vs 63-80 mm), and this identification must be rejected. Peters (1998) restudied the material seen by Gautier, accepting his identification as *C. thomasi*, and concluded that this species was morphologically identical to the domestic dromedary and might be considered its wild ancestor. Later authors accepted and reinforced his proposal (von den Driesch & Obermaier 2007). However, no morphological or metric comparison with the material from the type-locality of *C. thomasi* had ever been conducted, thus any discussion of the affinities of this species were lacking a sound basis. Our detailed study shows instead that *C. thomasi* differs clearly from both extant forms, rejecting other opinions found in the literature.

CONCLUSION

The material of *Camelus thomasi* from the type-locality Tighennif is sufficient to satisfactorily define the species, even though several bones remain unknown. Besides perhaps in the Thomas-Oulad Hamida cave complex in Morocco, there is no published convincing evidence of this species elsewhere. The hypothesis that *C. thomasi* was a widespread species from which the modern dromedary derives is not supported by the current morphological evidence.

The history of fossil camels in Afro-Arabia and the Near East remains poorly documented; hopefully, recently collected material from Syria and Ethiopia will shed new light on their evolution.

Acknowledgements
We are grateful to C. Argot and J. Lesur (MNHN), G. Baryshnikov (ZIN), D. Berthet (CCEC), D. Lefèvre and J.-P. Raynal (CNRS), B. Oberholzer and M. Haffner (ZM), P. Schmid (NMBE), J. Studer (MHNG), M. Podestà and G. Bardelli (MSNM), and L. Costeur (NMB) for access to collections, to P. Loubry for the photos of *C. thomasi* in the MNHN, and to Y. Chaïd-Saoudi for photos of the Algiers material. Thanks also to the reviewers, J. Morales and J. van der Made, for their helpful comments.

REFERENCES

Arambourg C. & Hoffstetter R. 1963. — Le gisement de Ternifine. *Archives de l'Institut de Paléontologie humaine* 32: 1-190.
Gautier A. 1966. — *Camelus thomasi* from the Northern Sudan and its bearing on the relationship *C. thomasi-C. bactrianus*. *Journal of Paleontology* 40 (6): 1368-1372.
Geraads D. 2016. — Pleistocene Carnivora (Mammalia) from Tighennif (Ternifine), Algeria. *Geobios* 49: 445-458. https://doi.org/10.1016/j.geobios.2016.09.001
Geraads D. & Bernoussi R. 2017. — La faune de vertébrés du Pléistocène moyen de la Grotte des Rhinocéros, Casablanca, Maroc : 6 – Hippopotamidae, Suidae and Camelidae, *in* Raynal J.-P. & Mohib A. (eds), *Préhistoire de Casablanca 1 – La Grotte des Rhinocéros (fouilles 1991 et 1996).* NSAP, Rabat, Villes et Sites archéologiques du Maroc 6: 133-134.
Geraads D., Hublin J.-J., Jaeger J.-J., Tong H., Sen S. & Toubeau P. 1986. — The Pleistocene Hominid site of Ternifine, Algeria: new results on the environment, age and human industries. *Quaternary Research* 25: 380-386. https://doi.org/10.1016/0033-5894(86)90008-6
Gray J. E. 1821. — On the natural arrangment of vertebrose animals. *London Medical Repository* 15: 296-310.
Grigson C. 1983. — A very large camel from the Upper Pleistocene of the Negev desert. *Journal of Archaeological Science* 10: 311-316. https://doi.org/10.1016/0305-4403(83)90068-7
Harris J. M., Geraads D. & Solounias N. 2010. — 41 – Camelidae, *in* Werdelin L. & Sanders W. J. (eds), *Cenozoic Mammals of Africa*. University of California Press, Berkeley: 815-820.
Hublin J.-J. 2001. — Northwestern African Middle Pleistocene hominids and their bearing on the emergence of *Homo sapiens*, *in* Barham L. & Robson-Brown K. (eds), *Human Roots. Africa and Asia in the Middle Pleistocene*. Western Academic and Specialist Press, Bristol: 99-121.
Lhote H. 1987. — *Chameau et Dromadaire en Afrique du Nord et au Sahara : Recherches sur leurs Origines.* Office national des approvisionnements et des services agricoles (ONAPSA), Alger, Algeria, 161 p.
Linnæus C. 1758. — *Systema naturæ per regna tria naturæ, secundum classes, ordines, genera, species, cum characteribus, differentiis, synonymis, locis. Tomus I.* Editio decima, reformata. Salvii, Stockholm, 824 p. https://doi.org/10.5962/bhl.title.542
Martini P., Schmid P. & Costeur L. J. 2017. — Comparative morphometry of Bactrian camel and Dromedary. *Journal of Mammalian Evolution*. https://doi.org/10.1007/s10914-017-9386-9
Martinón-Torres M., Bermúdez de Castro J.M., Gómez-Robles A., Arsuaga J. L., Carbonell E., Lordkipanidze D., Manzi G. & Margvelashvili A. 2007. — Dental evidence on the hominin dispersals during the Pleistocene. *Proceedings of the National Academy of Sciences of the USA* 104: 13279-13282. https://doi.org/10.1073/pnas.0706152104
Morales J., Pickford M. & Soria D. 1993. — Pachyostosis in a Lower Miocene giraffoid from Spain, *Lorancameryx pachyostoticus* nov. gen. nov. sp. and its bearing on the evolution of bony appendages in artiodactyls. *Geobios* 26: 207-230. https://doi.org/10.1016/S0016-6995(93)80016-K
Peters J. 1998. — *Camelus thomasi* Pomel, 1893, a possible ancestor of the one-humped camel? *Zeitschrift für Säugetierkunde* 63: 372-376. https://biodiversitylibrary.org/page/45538035
Pomel A. 1886. — Station préhistorique de Ternifine (Mascara). *Comptes rendus de l'Association française pour l'Avancement des Sciences* 14: 504-505. http://gallica.bnf.fr/ark:/12148/bpt6k2011635/f507.image
Pomel A. 1893. — *Paléontologie – Monographies – Caméliens et Cervidés.* Carte géologique de l'Algérie, Alger, Algeria, 50 p.
Sahnouni M. & van der Made J. 2009. — The Oldowan in North Africa within a biochronological framework, *in* Schick K. & Toth N. (eds), *The Cutting Edge: new Approaches to the Archaeology of Human Origins.* Stone Age Institute Press, Gosport: 179-210.

STEIGER C. 1990. — *Vergleichend morphologische Untersuchungen an Einzelknochen des postkranialen Skeletts der Altweltkamele.* Dissert. Ludwig-Maximilians Univ. München, 106 p.

VON DEN DRIESCH A. & OBERMAIER H. 2007. — *The Hunt for Wild Dromedaries during the 3rd and 2nd Millennia BC on the United Arab Emirates Coast. Camel Bone Finds from the Excavations at Al Sufouh 2, Dubai, UAE.* Skeletal Series and their Socio-economic Context. J. Grupe and J. Peters.

WOODWARD A. S. 1921. — A New Cave Man from Rhodesia, South Africa. *Nature* 108: 371-372. https://doi.org/10.1038/108371a0

Submitted on 12 May 2017;
accepted on 6 October 2017;
published on 15 March 2018.

APPENDIX 1. — Cranial measurements of *Camelus thomasi* Pomel, 1893, compared to the extant species *C. bactrianus* Linnaeus, 1758 and *C. dromedarius* Linnaeus, 1758 (data from Martini *et al.* 2017). Abbreviations: **Min**, minimal measurement; **Max**, maximal measurement; **N**, number of individuals. Data in mm. Data in **red** font are approximate measurements; *, see remarks in the text.

		C. bactrianus				*C. dromedarius*				TER 1689	TER 1816
Cranium		**Min**	**Average**	**Max**	**N**	**Min**	**Average**	**Max**	**N**	**(sin)**	**(sin)**
C1	Maximal length (prosthion to akrokranion)	491	539.1	579	17	462	499.9	534	13	575 *	–
C5	Occipital height (akrokranion to opisthion)	60	70.8	82	17	55	61.9	70	14	70	–
C6	Length of foramen magnum (opisthion to basion)	36	39.9	43	17	36	39.5	42	14	37	–
C8	Basicranial length (basion to staphilion)	164	185.2	202	17	144	160.1	170	14	190	–
C9	Basal length (basion to prosthion)	428	473.6	512	12	409	439.2	461	10	490	–
C10	Palatal length (staphilion to prosthion)	262	288.2	311	17	260	284.4	300	11	305	–
C11	Shorter palatal length (staphilion to intermaxillare)	199	221.1	233	11	192	216.9	232	9	243	
C12	Lateral postorbital length (orbita to akrokranion)	232.5	265.9	295.5	17	218	239.8	255.5	14	295	–
C13	Lateral preorbital length (orbita to prosthion)	240	261.1	278	17	228.5	251.7	274.5	13	272	–
C14	Cheek length (predentale to orbita)	112	119.1	131	16	97	107.8	123	13	127	111
C15	Infraorbital length (infraorbital foramen to orbita)	59	71.5	81	16	49	56.9	67.5	14	70	65
C18	Orbital length (maximal horizontal diameter)	59	64.0	67	16	55.5	58.3	61.5	14	77	–
C22	Distance from zygomatic process of temporal to orbita	16	21.6	27.5	14	18	23.1	29	11	24	–
C23	Transversal thickness of zygomatic arch	8.5	11.7	17	14	6	7.3	11	11	12	–
C24	Suborbital height (orbita to M3 distal)	56	72.7	83	15	48	59.1	68.5	13	66	55
C25	Position of palatine foramina (from staphylion)	40	67.4	85.5	16	88	100.1	120	14	107	–
C26	Position of incisive (prosthion to incisive, rostral)	34	38.5	46.5	15	30	34.5	40	12	23	–
C27	Position of canine (prosthion to canine, rostral)	57.5	63.8	74	15	56.5	60.1	63	13	58	–
C28	Position of P1 (prosthion to P1, rostral)	97.5	119.9	131	15	90	100.1	113	12	106	–
C29	Position of cheek tooth (prosthion to P3, rostral)	145.5	161.6	183	16	139	153.4	163	12	168	–
C30	Position of M1 (prosthion to M1, rostral buccal)	177	202.7	228	13	174	193.3	211	11	215	–
C31	Postdental position (prosthion to M3 distal	303.5	320.9	340	11	264.5	295.6	319	10	330	–
C32	Oral length (prosthion to uranion)	306.5	328.8	344.5	12	274.5	302.9	324	10	343	–
C33	Cheek tooth length (P3-M3, included; buccal side)	135.5	158.5	175	14	128	144.2	157.5	13	161	140.5
C34	Molar row length (M1-M3, included; buccal side)	103	116.4	123.5	14	90.5	102.8	111	13	114	102
C35	Basidental length (basion-P3, rostral)	284.5	316.3	345	12	268	288.2	303	11	325	–
C45	Maximal diameter of condyle	53.5	58.6	68.5	17	52	56.0	62.25	12	60	–
C46	Breadth of glenoid fossa (maximal)	50	58.0	69	14	44	49.6	53	9	72	–
C51	Breadth of nasal opening (between nasointermaxillares)	27	31.8	36	16	23	36.4	46	12	50	–
C52	Breadth between infraorbital foramina (lateral border)	88	96.5	108	16	83	88.9	95	14	101	–
C54	Minimal biorbital breadth (between medial borders)	163	181.2	207	17	149	164.4	178	13	225	–
C56	Breadth of postorbital constriction (minimal)	80	90.2	102	17	74	80.4	88	14	120	–
C57	Breadth of the braincase (maximal)	112	123.5	136	17	95	101.0	110	13	131	–
C58	Breadth between squamotemporal foramina	116	123.3	132	12	96	107.0	115	9	121	–
C59	Breadth between incisors (rostral)	36	47.1	64	16	38	44.5	57	11	50	–
C60	Breadth between canines (rostral)	44	54.4	81	16	42	49.7	67	13	59	–
C62	Breadth between P3's (rostral)	44	55.7	70	16	46	50.5	57	14	60	52
C63	Breadth between M1's (rostral, buccal side)	83	103.5	121	16	86	92.5	104	13	117	116
C64	Breadth between postdentales (M3 distal)	114	129.5	148	14	107	114.9	126	11	133	112
C73	Maximal bicondylar breadth	74	81.8	92	17	78	82.9	91	13	97	–
C74	Minimal bicondylar breadth	37.5	43.5	50.5	17	40	45.6	51	11	45	–
C75	Breadth of foramen magnum (between condyles)	28	35.0	41	17	30	34.1	39	13	35	–

APPENDIX 1. — Continuation.

Mandibula		*C. bactrianus* Min	Average	Max	N	*C. dromedarius* Min	Average	Max	N	TER 1683 (sin)	TER 1684 (dex)	TER 1685 (dex)	TER 1686 (dex)	TER 1687 (sin)	TER 1688 (dex)	TER 1900-27 (sin)
M7	Length from p4 to m3 distal	146.5	163.0	186	11	121	138.0	150.5	11	126	–	161	–	–	–	–
M11	Position of caudal mental foramen: from p4 mesial to caudal mental foramen	33.5	43.9	65	11	42.5	55.9	69	11	58	–	–	–	–	–	–
M12	Length from p4 mesial to angular process	267	285.1	301	11	234	251.6	271	11	220	–	275	–	–	–	–
M13	Length from m3 distal to angular process	101	124.0	141.5	11	95.5	114.4	129	11	99	–	117	–	–	–	–
M14	Length from m3 distal to condylar process	106.5	134.2	158.5	11	108	122.8	132.5	9	100	–	121	–	–	–	–
M15	Thickness of the corpus measured between m1 and m2	32.5	36.1	40.5	11	27	30.5	35	11	35.5	35	40	–	–	34	43
M16	Thickness of the corpus measured between m2 and m3	37.5	40.5	45.5	11	32.5	36.5	40	11	41	42	51	51	48	39	48
M17	Breadth of the condylus	42	48.1	52.5	11	39.25	41.8	45.25	9	–	–	39	–	–	–	–
M19	Height of the corpus mesial to p4	36	40.7	49.5	11	36.5	40.7	48	11	32	–	48	–	–	–	–
M20	Height of the corpus between m1 and m2	41	53.8	60	11	47.5	55.3	59.5	11	37	36	39.5	–	39	43	43
M21	Height of the corpus distal to m3	65	76.2	86.5	11	72.5	80.3	86.5	11	65	65	72	85	78	74	–
M22	Height of the ramus from coronoid process to ventral border	222	244.5	259	11	199	209.5	221	11	189	191	230	–	–	–	–
M23	Height of the ramus from rostral notch to ventral border	153	170.2	182	11	150.5	160.9	173.5	11	127	136	160	–	–	–	–
M24	Height of the ramus from condylar process to ventral border	166	186.8	199.5	11	171	179.7	189.5	9	–	–	181	–	–	–	–
M25	Height of the ramus from caudal notch to ventral border	117	139.4	152	11	123	132.3	143	11	102	–	138	–	–	–	–

Upper teeth		*C. bactrianus* Min	Average	Max	N	*C. dromedarius* Min	Average	Max	N	TER 1689 (sin)	OH1-GDR F14-87	TER 1816
Ds1	Alveolar length of I3	7	10.9	20	11	9	13.4	18	9	17	–	–
Ds2	Alveolar breadth of I3	6	9.3	16.5	11	8	9.8	13	8	15	–	–
Ds3	Alveolar length of C	11	16.7	29	11	11	18.7	26	9	35	–	–
Ds4	Alveolar breadth of C	9	13.9	25	11	9.5	14.3	20	8	21	–	–
Ds7	Alveolar length of P3	16	19.6	24	10	15	18.6	24	10	20	–	16
Ds8	Alveolar breadth of P3	15	19.7	24	9	15	17.3	19	9	20	–	–
Ds9	Occlusal length of P3	16	17.9	20	9	14.5	16.5	19	9	20	–	18
Ds10	Occlusal breadth of P3	9.5	12.7	18.5	9	10	12.0	15	9	13	–	–
Ds11	Alveolar length of P4	19	21.6	23.5	8	18	21.6	24	10	22	–	21
Ds12	Alveolar breadth of P4	23	25.9	29	9	23	24.9	27	9	28	–	25
Ds13	Occlusal length of P4	22	24.0	26	9	20	22.7	25	10	22	–	20
Ds14	Occlusal breadth of P4	18	20.3	24	9	16	18.6	20.5	9	17	–	21
Ds15	Alveolar length of M1	24	28.2	32.25	9	23.75	27.6	32	10	26	29	24
Ds16	Alveolar breadth of mesial lobe of M1	28.5	30.8	34	10	26	29.4	33	9	33	35	29
Ds17	Alveolar breadth of distal lobe of M1	26	30.7	35	10	26	30.1	34	9	31	33	33
Ds18	Occlusal length of M1	27.75	37.1	41	10	28	32.9	42	10	36	36	30
Ds19	Occlusal length of mesial lobe of M1	15.5	19.0	23	10	12	16.7	20	10	18	18	–
Ds20	Occlusal length of distal lobe of M1	13	18.6	21.5	10	13.25	16.6	22	10	19	18	–
Ds21	Occlusal breadth of mesial lobe of M1	24	26.8	30.5	10	23	25.6	28	9	22.5	–	–
Ds22	Occlusal breadth of distal lobe of M1	22	24.2	28.5	10	20	23.9	27	9	20	24	28
Ds23	Alveolar length of M2	32.5	39.1	44.5	10	26	34.7	42	10	37	33	33
Ds24	Alveolar breadth of mesial lobe of M2	28.5	32.1	36	10	27	30.6	34	9	34.5	34	35
Ds25	Alveolar breadth of distal lobe of M2	25	29.1	33	10	23	27.9	32	7	26	28	30.5
Ds26	Occlusal length of M2	39.5	47.4	52	10	34	40.3	48	10	47	38	36

APPENDIX 1. — Continuation.

Upper teeth (continuation)	*C. bactrianus* Min	Average	Max	N	*C. dromedarius* Min	Average	Max	N	TER 1689 (sin)	OH1-GDR F14-87	TER 1816
Ds27 Occlusal length of mesial lobe of M2	21	24.6	27	10	17.25	20.7	23	10	27	20	20
Ds28 Occlusal length of distal lobe of M2	19.5	24.3	28	10	17	21.0	26	10	23.5	20	21
Ds29 Occlusal breadth of mesial lobe of M2	24	26.6	30.25	10	22	24.9	26	9	23	24	25
Ds30 Occlusal breadth of distal lobe of M2	19.5	22.1	26.5	10	18	21.5	23.75	9	18	19	22
Ds31 Alveolar length of M3	39.5	46.1	51	10	36	41.6	46	9	44	–	40
Ds32 Alveolar breadth of mesial lobe of M3	25	29.7	34	10	23	28.4	32	8	26	–	32
Ds33 Alveolar breadth of distal lobe of M3	21	24.7	30	10	18	22.3	26	9	22	–	29
Ds34 Occlusal length of M3	45	47.3	51.5	10	35	40.9	47	10	43	–	43
Ds35 Occlusal length of mesial lobe of M3	22.5	25.2	28	10	20	22.0	25	10	22	–	23
Ds36 Occlusal length of distal lobe of M3	19	23.0	25	10	12	19.8	24	10	22	–	23
Ds37 Occlusal breadth of mesial lobe of M3	21	24.0	27.75	10	16	22.5	25.5	8	19	–	24
Ds38 Occlusal breadth of distal lobe of M3	16	18.9	22.5	10	11	16.9	20	8	14	–	19.5

Lower teeth	*C. bactrianus* Min	Average	Max	N	*C. dromedarius* Min	Average	Max	N	TER 1683 (sin)	TER 1684 (dex)	TER 1685 (dex)	TER 1686 (dex)	TER 1687 (sin)	TER 1688 (dex)	TER 1900-27 (sin)
Di8 Alveolar length of P4	18	19.8	23	9	17	18.9	21	8	–	–	24	–	–	–	–
Di9 Alveolar breadth of P4	13	14.6	18	9	11	12.7	14	8	–	–	15	–	–	–	–
Di10 Occlusal length of P4	20	22.8	25	8	18	19.4	23	8	–	–	22	–	–	–	–
Di11 Occlusal breadth of P4	11	13.8	16	9	9	11.3	13	8	–	–	13	–	–	–	–
Di12 Alveolar length of M1	23	26.7	28.5	9	22.5	25.4	27	8	–	–	30	–	–	–	–
Di13 Alveolar breadth of mesial lobe of M1	17	19.2	22	9	14.5	17.4	21	8	–	–	23	–	–	–	–
Di14 Alveolar breadth of distal lobe of M1	19.5	20.8	24	9	17	20.1	23	8	–	–	23	–	–	–	–
Di15 Occlusal length of M1	27	32.1	38	9	25.5	30.5	38	8	–	–	34	–	–	–	–
Di16 Occlusal length of mesial lobe of M1	11.5	15.4	21	8	11	14.6	19	8	–	–	15	–	–	–	–
Di17 Occlusal length of distal lobe of M1	15	17.8	20	8	12	15.9	19	8	–	–	19	–	–	–	–
Di18 Occlusal breadth of mesial lobe of M1	17.5	19.2	21	9	16	17.9	19.25	8	–	–	18	–	–	–	–
Di19 Occlusal breadth of distal lobe of M1	19.5	21.2	23.5	9	18	19.9	22	8	–	–	20	–	–	–	–
Di20 Alveolar length of M2	32	38.9	47	9	26.5	33.7	42	8	28	30	40	–	–	–	34
Di21 Alveolar breadth of mesial lobe of M2	22	24.2	26	9	19	21.7	24	8	24	24	26	–	–	–	27
Di22 Alveolar breadth of distal lobe of M2	22	24.3	27	9	19.25	22.5	25	8	25	25	25.5	–	26	–	27.5
Di23 Occlusal length of M2	36.75	44.0	48	9	33.5	39.4	45.5	8	35	35	44	–	–	–	37
Di24 Occlusal length of mesial lobe of M2	17	20.8	22.75	9	16.5	19.3	22	8	17	16	19.5	–	–	–	16
Di25 Occlusal length of distal lobe of M2	20	23.3	26	9	17.75	20.3	23.5	8	18.5	18.5	25	–	–	–	19
Di26 Occlusal breadth of mesial lobe of M2	18	20.9	23.25	9	15.5	18.9	21	8	24	25	20	–	–	–	25
Di27 Occlusal breadth of distal lobe of M2	19	21.2	24	9	16	19.6	21.75	8	24	24.5	21	–	–	–	25
Di28 Alveolar length of M3	50	55.7	59	9	47	50.2	57	8	46	48	58	51	55	52	57
Di29 Alveolar breadth of mesial lobe of M3	20	23.3	26	9	18	21.7	24	8	24	24.5	23	27	25	26	28
Di30 Alveolar breadth of central lobe of M3	18.75	23.3	26	9	16	20.6	22.5	8	23	23	24	26.5	24	26	25
Di31 Alveolar breadth of distal lobe of M3	8.75	13.0	16	9	9	12.0	14	8	11.5	13	14	14	14	15	13.5
Di32 Occlusal length of M3	49.5	54.4	60.5	9	45	49.3	55	8	45	46	48	–	–	–	57
Di33 Occlusal length of mesial lobe of M3	19	22.6	26.25	9	18.5	20.6	23	8	18	18	20	–	–	–	20
Di34 Occlusal length of central lobe of M3	18	21.6	26	9	15.5	19.8	22	8	17	18	20	–	–	–	–
Di35 Occlusal length of distal lobe of M3	10.5	13.2	15	8	6	10.9	14.5	8	11.5	11	11	–	–	–	–
Di36 Occlusal breadth of mesial lobe of M3	15	18.7	23	9	13	17.8	20	8	21	20.5	18	–	–	–	24
Di37 Occlusal breadth of central lobe of M3	15	19.3	23	9	9	16.1	20	8	21	20.5	17	–	–	–	–
Di38 Occlusal breadth of distal lobe of M3	6.5	9.9	13.5	8	8.5	10.6	12	7	10	10	8	–	–	–	–

APPENDIX 2. — Measurements of long bones, metapods and phalanges in *Camelus thomasi* Pomel, 1893, compared to the extant species *C. bactrianus* Linnaeus, 1758 and *C. dromedarius* Linnaeus, 1758 (data from Martini *et al.* 2017). Abbreviations: **Min**, minimal measurement; **Max**, maximal measurement; **N**, number of individuals. Data in mm; data in **red** font are approximate measurements; data in **blue** font are measurements that might be either mesial or lateral.

		C. bactrianus				*C. dromedarius*				TER 1649	TER 1650	TER 1682
Tibia		**Min**	**Average**	**Max**	**N**	**Min**	**Average**	**Max**	**N**	**(sin)**	**(dex)**	**(dex)**
ti2	Length axial (from epicondylar eminence)	413.5	442.7	493	11	415.5	449.8	487	10	–	–	535
ti3	Length lateral (condyle to lateral fossa)	368	392.5	439.5	12	365.5	404.6	440	10	–	–	500
ti5	Depth of the lateral condyle	38	43.0	50	12	36.5	40.2	43.5	10	–	–	51
ti8	Breadth of the lateral condyle	59	64.7	68	10	54	60.7	65	6	–	–	62
ti12	Minimal depth of the diaphysis	25	29.8	34	12	25.5	28.1	31	10	35	–	33
ti13	Minimal breadth of the diaphysis	45	50.7	54.75	12	41.75	44.4	48.5	9	–	–	51
ti14	Depth of the medial fossa of the cochlea (maximal)	40.25	46.9	52	12	43	44.7	47	10	45	41	–
ti15	Depth of the axial fossa of the cochlea (maximal)	41.75	46.0	52	12	38.5	45.2	50	10	46	–	43
ti16	Depth of the lateral fossa of the cochlea	38	40.4	46	12	31.25	35.5	38	11	41	–	46
ti17	Dorsal breadth of the cochlea	75.5	81.6	91	12	70.5	77.3	83	11	87	88	–
ti18	Palmar breadth of the cochlea	79.75	86.7	95.5	12	74.25	82.4	89	11	97.5	–	–
ti19	Breadth of the medial fossa of the cochlea	33	35.4	38	10	31	32.3	34	4	29	27	–
ti20	Breadth of the axial fossa of the cochlea	21.5	24.6	27	10	21	23.8	25	4	25	26	–
ti21	Breadth of the lateral fossa of the cochlea	19	20.3	21	10	15	16.5	18	4	20	–	20

		C. bactrianus				*C. dromedarius*				TER 1647	TER 1648						TER 1681
Metacarpale		**Min**	**Average**	**Max**	**N**	**Min**	**Average**	**Max**	**N**	**(sin)**	**(dex)**	**TER 1652**	**TER 1653**	**TER 1654**	**TER 1659**	**TER 1661**	**(sin)**
mp1	Length on the medial side	296	323.3	352	13	327	348.8	385	15	–	420	–	–	–	–	–	–
mp2	Length on the lateral side	295	322.8	353.5	13	329	349.6	389.5	15	–	400	–	–	–	–	–	–
mp3	Medial depth of the proximal articulation	46	49.0	56.75	13	43.5	47.5	53	15	62	51	–	–	–	–	56	54
mp4	Lateral depth of the proximal articulation	42.75	46.5	55.75	13	39	43.8	48	15	–	–	–	–	–	–	53	50
mp5	Breadth of the proximal articulation	67.5	74.2	84.75	13	62.5	70.9	78	15	–	78	–	–	–	–	79	85
mp6	Breadth of the medial proximal facet	31	33.8	38	11	25	31.6	36	7	41	–	–	–	–	–	34	–
mp7	Breadth of the lateral proximal facet	20	26.3	32	11	21.5	26.8	30	7	–	–	–	–	–	–	31	–
mp8	Depth of the proximal articulation	42	46.0	55	11	40	45.6	49	8	–	–	–	–	–	–	52	50
mp9	Depth of the medial proximal facet	40	45.3	51	11	40	44.7	47	7	56	–	–	–	–	–	50	–
mp10	Maximal depth of the diaphysis	29	34.1	42	13	28.5	33.7	40	15	–	41	38	–	–	–	–	–
mp11	Minimal depth of the diaphysis	20	22.8	25.75	13	20.5	22.2	25.5	15	–	26	23	28	24	–	–	32
mp12	Minimal breadth of the diaphysis	33	38.7	44	13	32.25	35.8	39	15	–	47	41	–	–	–	–	48
mp13	Depth of the medial condyle	40	42.7	47.75	13	40	42.9	47	15	–	–	41 *	44	44	56	–	–
mp14	Depth of the lateral condyle	38.5	41.5	47.75	13	40.5	42.8	45	15	–	49	41 *	–	44	56	–	–
mp15	Breadth of the medial condyle	40	43.9	49.5	13	36.75	42.2	46.5	15	–	42	55 *	42	44	52	–	–
mp16	Breadth of the lateral condyle	39.5	44.9	53	13	38	42.6	48	15	–	44	55 *	44	44	52	–	–
mp17	Maximal distal breadth	88.25	96.2	110	13	83	92.2	102	15	–	89	–	99	91.5	–	–	–

APPENDIX 2. — Continuation.

Metatarsale		*C. bactrianus* Min	Average	Max	N	*C. dromedarius* Min	Average	Max	N	TER 1651 (dex)	TER 1655 (sin)	TER 1656 (dex)	TER 1657 (dex)	TER 1658 (dex)	TER 1662 (dex)	TER 1663 (sin)	TER 1664 (dex)	TER 1690 (sin)
mp1	Length on the medial side	305	330.9	362.5	13	338	356.4	378	11	–	–	–	–	–	–	–	420	415
mp2	Length on the lateral side	304.5	333.0	363.5	13	340	358.8	381	11	–	–	–	–	–	–	–	410	–
mp18	Length of the triangular process	18	22.9	28	12	22	26.5	31.75	11	–	–	25.5	–	–	–	–	–	27
mp19	Breadth of the triangular process	17	24.0	30.5	13	14.25	20.2	29	11	–	29	31	26	–	–	–	–	32
mp20	Depth of the medioplantar proximal facet	12.5	14.8	17	13	11	13.4	16	11	–	18	23	20	18.5	16	–	–	19
mp21	Depth of the medial proximal facet	28.5	31.9	35.5	13	28	30.4	34.5	11	–	36	33	34	39	33	–	38	33
mp22	Depth of the lateral proximal facet	34.5	39.8	46.75	13	35	38.3	40.5	11	–	44	45	42	46	43	–	–	43
mp5	Breadth of the proximal articulation	59	63.3	74.5	13	54.5	59.8	64	11	–	68	71	70	80	67	74	63	67
mp6	Breadth of the medial proximal facet	20	21.7	24	10	18	20.9	24	5	–	25	23.5	22	30.5	27.5	–	25	25
mp7	Breadth of the lateral proximal facet	18	20.9	24	10	17	19.8	21	5	–	27	27	26	29	28	–	–	24
mp8	Depth of the proximal articulation	45	49.3	53	10	45.75	49.0	56	6	–	57.5	55	52	59	51	–	56.5	54
mp10	Maximal depth of the diaphysis	30	34.8	39.5	13	31	35.2	41	11	–	–	–	–	–	41	43.5	42	40
mp11	Minimal depth of the diaphysis	19.5	22.6	26	13	19	21.3	24	11	22.5	–	–	–	–	–	–	26	26.5
mp12	Minimal breadth of the diaphysis	27.5	33.3	41	13	27.5	29.4	32.5	11	–	–	–	–	–	35	37	36	35
mp13	Depth of the medial condyle	35	36.6	40	13	34	36.3	39	11	40	–	–	–	–	–	–	–	–
mp14	Depth of the lateral condyle	36	38.1	44	13	33	37.1	41.25	11	41.5	–	–	–	–	–	–	38	–
mp15	Breadth of the medial condyle	34.5	37.1	41.75	13	31.75	35.0	38	11	40	–	–	–	–	–	–	–	–
mp16	Breadth of the lateral condyle	35	38.9	45.5	13	31.5	34.8	39	11	40	–	–	–	–	–	–	36	–
mp17	Maximal distal breadth	78	83.6	94	13	71.5	76.8	85	11	89	–	–	–	–	–	–	77	–

Phalanx proximal anterior		*C. bactrianus* Min	Average	Max	N	*C. dromedarius* Min	Average	Max	N	TER 1674	TER 1675	TER 1676	TER 1677
pp1	Length of the axial side	96	102.1	–	9	92.5	102.7	–	13	122	126	120	126
pp2	Length of the abaxial side	94.5	99.4	108	9	91	100.4	–	13	120	–	117	123
pp3	Proximal depth (articular surface)	34.5	36.0	40.75	9	31	35.3	39.5	13	43	43	40	43
pp4	Proximal breath (articular surface)	43.5	45.7	50.25	9	35.5	42.0	–	13	53	51	52	54
pp5	Depth of the diaphysis	17	18.8	22	9	17	18.3	20.25	13	22.5	22.5	22.5	23
pp6	Breadth of the diaphysis	17.5	22.0	26.75	9	18	21.0	–	13	27	27	29	29
pp7	Depth of the condyle	22.75	25.4	29.75	9	23.5	25.2	28.5	13	31.5	31.5	31	35
pp8	Breadth of the condyle	36	40.8	47.25	9	36.5	40.9	46.5	8	46	46	45	44
pp9	Length of the axial lip of the condyle	28	31.5	35.25	9	31.25	34.7	–	9	40	40	38	40.5
pp10	Length of the abaxial lip of the condyle	31.5	34.7	41	9	32	37.0	41.5	10	42	39	40	42

Phalanx proximal posterior		*C. bactrianus* Min	Average	Max	N	*C. dromedarius* Min	Average	Max	N	TER 1673
pp1	Length of the axial side	85.75	90.9	99	8	85	91.8	97.5	11	103
pp2	Length of the abaxial side	85.25	89.5	97.75	8	83	90.2	96.5	11	103
pp3	Proximal depth (articular surface)	29	30.5	34.5	8	28	29.8	33.75	11	33
pp4	Proximal breath (articular surface)	37	39.5	43.75	8	33	36.0	40	11	41
pp5	Depth of the diaphysis	14.5	16.6	21.25	8	13.5	15.4	17	11	17
pp6	Breadth of the diaphysis	17.5	19.9	23	8	16.5	18.6	22	11	21.5
pp7	Depth of the condyle	19.75	22.4	26.5	8	19	22.1	26	11	24
pp8	Breadth of the condyle	32	34.9	39	8	30	33.9	40	10	34.5
pp9	Length of the axial lip of the condyle	25.25	27.2	30.5	8	26	28.9	32	10	32
pp10	Length of the abaxial lip of the condyle	27	30.4	34.25	8	29	32.4	37	10	33

APPENDIX 3. — Measurements of short bones (carpals and tarsals) in *Camelus thomasi* Pomel, 1893, compared to the extant species *C. bactrianus* Linnaeus, 1758 and *C. dromedarius* Linnaeus, 1758 (data from Martini *et al.* 2017). Abbreviations: **Min**, minimal measurement; **Max**, maximal measurement; **N**, number of individuals. Data in mm. Data in **red** font are approximate measurements.

		C. bactrianus				*C. dromedarius*				
Trapezoideum		**Min**	**Average**	**Max**	**N**	**Min**	**Average**	**Max**	**N**	**Unlabeled**
Kt1	Maximal height	23.5	26.0	30	11	23.5	26.3	29	9	19
Kt2	Maximal diagonal	25	28.8	35	11	22.5	28.6	33.75	10	25
Kt3	Maximal diameter of the distal facet	20	22.8	27.25	11	19	23.6	28	10	24
Kt4	Breadth of the proximal facet	19.5	21.0	24	10	17	19.6	24	10	16
Kt5	Minimal diameter of the distal facet	15	17.1	21	11	14	16.1	18	10	13

		C. bactrianus				*C. dromedarius*				
Fibula		**Min**	**Average**	**Max**	**N**	**Min**	**Average**	**Max**	**N**	**TER1660 (sin)**
fi1	Height dorsal	29.5	35.4	41.5	11	29.5	31.6	33.5	6	39
fi2	Height in the middle (height of the process)	27	31.2	36	11	24.25	29.5	31.5	7	36
fi4	Maximal depth	43	45.8	53.5	11	36.5	39.7	42.25	7	52
fi5	Depth of the proximal facet	37	40.3	47	11	32	34.9	37.5	7	43.5
fi6	Depth of the distal facet	31.5	36.9	42	11	30.5	32.9	35	7	38
fi7	Dorsal breadth of the proximal side	23.75	27.8	34.5	11	22	24.3	27	6	32
fi8	Plantar breadth of the proximal facet	14.5	19.8	22.25	11	13	15.5	17	7	25
fi9	Breadth of the distal facet	19	21.5	24.5	11	17.5	18.6	19.5	7	25
fi10	Depth of the medial (astragalar) facet	34	37.2	43	11	31	33.1	35	7	41

		C. bactrianus				*C. dromedarius*							
Talus		**Min**	**Average**	**Max**	**N**	**Min**	**Average**	**Max**	**N**	**TER1669 (dex)**	**TER1670 (dex)**	**TER1671 (sin)**	**TER1672 (dex)**
Ta1	Height of the lateral side	69.5	74.6	85	12	71	74.6	80	8	90	84	–	82
Ta2	Height axial	54	58.1	64.5	12	54.5	57.5	61	9	67	64.5	65	65
Ta3	Height of the medial side	64	69.1	76.75	12	62.5	66.2	71	8	80	76	76.5	77
Ta4	Proximal depth of the lateral side	29	31.1	36	12	27	31.0	34	9	36	34	–	36
Ta5	Distal depth of the lateral side	22.75	25.1	27.5	12	19	23.5	27	9	31	29	–	25
Ta6	Middle depth of the lateral side	33	36.0	41	12	31.5	35.1	40.5	8	43	42	–	41
Ta7	Proximal breadth	41	44.2	49	12	40	43.9	48	9	51	48	–	49
Ta8	Breadth of the calcaneal surface	29	32.4	37.75	12	25	28.8	34	9	36	35	34	32
Ta9	Breadth at the lateral (calcaneal) process	50.5	54.4	62	12	45	52.4	55.5	9	61	59	58	61
Ta10	Distal breadth	46.5	49.8	57.5	12	44	48.9	54	9	58	53	56	57
Ta11	Greater maximal diameter (dorsolateral-distomedial)	80	85.6	95.25	12	79.25	84.8	91	9	100	98	–	96
Ta12	Lesser maximal diameter (dorsomedial-distolateral)	74	78.4	87.75	12	73	76.2	83	9	90	85	87	87
Ta13	Minimal depth of the proximal trochlea (groove)	19	21.7	24	9	21	21.7	22	3	25.5	25	23	24.5
Ta14	Breadth of the medial part of the distal trochlea	29.5	32.6	36	9	27	29.3	32	4	37	34	34	–
Ta15	Breadth of the lateral part of the distal trochlea	15.25	18.1	22	9	20	20.8	21	4	22	20	21	–
Ta16	Medial depth of the distal trochlea	23	25.8	29	7	23	24.6	26.5	4	30	32	28.5	29
Ta17	Axial depth of the distal trochlea (groove)	17.75	18.5	20	9	18	18.3	19	4	22	21.5	21	19
Ta18	Lateral depth of the distal trochlea	23	26.3	31	9	23	24.0	25	4	30	29	–	25
Ta19	Height of the calcalneal surface	43.5	50.9	57	9	49	53.0	57	4	60	54	–	53

APPENDIX 3. — Continuation.

Calcaneus		*C. bactrianus* Min	*C. bactrianus* Average	*C. bactrianus* Max	*C. bactrianus* N	*C. dromedarius* Min	*C. dromedarius* Average	*C. dromedarius* Max	*C. dromedarius* N	TER1665 (dex)	TER1666 (sin)	TER1667 (dex)	TER1668 (sin)
Tc1	Maximal height (greatest length)	134.5	143.9	161.5	12	127.5	140.1	151	11	–	170	170	162
Tc2	Depth of the tubercle	45.5	47.9	53	12	38	45.3	49.5	11	–	52	–	46.5
Tc3	Maximal breadth of the tubercle	37.75	43.0	49	12	31.5	38.0	44	10	–	47	–	46.5
Tc4	Minimal breadth of the tubercle	20	24.3	28	12	15	19.5	25	11	24	31	31	26
Tc5	Depth medial (plantar border to substentaculum)	59	66.0	79.5	12	50	56.1	61	11	72	75	–	72
Tc6	Breadth of the substentaculum	40	45.2	51	12	33.5	40.3	48	11	50	50.5	52.5	49
Tc7	Medial distal height	69	74.1	83.5	12	64	68.5	72	10	80	83	85	77
Tc8	Depth lateral (plantar border to fibular trochlea)	65.5	71.1	83	12	55	62.8	68	11	75	75	–	72
Tc9	Height of the fibular trochlea	29	34.1	39.5	12	28	31.0	35	11	37	35	39	33
Tc10	Breadth of the fibular trochlea	18.5	20.5	24.5	12	15	18.1	20	10	21	21	25	20
Tc11	Distal lateral height (fibular trochlea to distal facet)	54	59.1	67.25	12	53.5	57.1	60	10	65	64	65	59
Tc12	Breadth of the plantar border	17	20.0	24.5	12	16	21.1	24	11	22	26	–	25
Tc13	Height of the distal (cuboid) facet	40	44.4	52	12	35	38.6	41.5	11	48.5	48	52	47
Tc14	Breadth of the distal (cuboid) facet	20.5	24.1	28.5	12	20	21.6	23	9	24.5	26	30	26

Cuboideum		*C. bactrianus* Min	*C. bactrianus* Average	*C. bactrianus* Max	*C. bactrianus* N	*C. dromedarius* Min	*C. dromedarius* Average	*C. dromedarius* Max	*C. dromedarius* N	Tig82-560 (sin)
Tq1	Dorsal height	33	36.8	43.75	12	27	31.6	37	10	41.5
Tq2	Medial height (proximal process to centrodistal medial facet)	27	31.4	35	11	25	30.7	37	9	37
Tq3	Plantar diagonal (proximal process to plantar tuberosity)	42	46.8	54	12	33	45.2	51	10	56
Tq4	Proximal depth (proximal dorsal border to plantar tuberosity)	58	63.3	74.5	12	51	59.1	66	10	74
Tq5	Distal depth (distal dorsal border to plantar tuberosity)	50.5	56.6	66.75	12	47	54.3	61	10	65
Tq6	Lateral depth (proximal dorsolateral border to plantar tuberosity)	51	54.8	65.5	12	40	50.6	58	10	62
Tq7	From the plantar border of the proximal facet, to the dorsal border of the distal facet	51	58.3	67.25	12	44.5	54.1	61	10	64.5
Tq8	From the dorsal border of the proximal facet, to the plantar border of the distal facet	49.5	54.9	65.25	12	46	50.4	56.5	10	62
Tq9	Depth of the proximal facet	49.5	53.9	61	12	45	49.7	54.5	10	60
Tq10	Depth of the distal facet	32.5	39.2	45.75	12	35	37.8	41	10	43
Tq11	Length of the lateral groove (laterodorsal border of the proximal facet to distal facet)	37.5	42.8	51	12	36	40.6	44	9	48
Tq12	Length of the plantar tubercle (centrodistal medial facet to plantar tuberosity)	32	36.7	47.25	12	30	34.0	38	9	42
Tq13	Proximal breadth (centrodistal medial facet to lateral border of proximal facet)	44	49.3	59	12	37	44.4	50	9	52
Tq14	Distal breadth (centrodistal medial facet to lateral border of distal facet)	37	42.8	49	12	31.5	38.3	44	9	46
Tq15	Maximal diagonal breadth (proximal process to lateral border of distal facet)	45	49.9	56	12	37	47.8	54.5	10	60

APPENDIX 3. — Continuation.

Cuboideum (continuation)		*C. bactrianus* Min	Average	Max	N	*C. dromedarius* Min	Average	Max	N	Tig82-560 (sin)
Tq16	Breadth of the main proximal facet	33.5	37.2	43	12	28	33.9	39	9	42
Tq17	Breadth of the distal facet	24.5	27.5	37.5	12	22	24.8	28.5	9	29
Tq18	Breadth of the dorsal proximal facet	17	19.6	22.75	12	16	20.3	23.25	10	20

Naviculare		*C. bactrianus* Min	Average	Max	N	*C. dromedarius* Min	Average	Max	N	TER1678 (dex)	TER1679 (dex)
Tn1	Dorsal height	18	20.8	24	12	16	19.3	24	9	22	23
Tn2	Lateral height	14	17.0	21.25	12	14.25	16.2	18	8	19.5	20
Tn3	Plantar height	30.5	33.3	40	12	29	30.7	33.5	9	33	38
Tn4	Maximal depth	46	48.8	55.25	12	46	47.6	50	9	54	61.5
Tn5	Maximal breadth	32	34.6	40	12	26	28.9	31.5	9	41.5	42
Tn6	Depth of the distal dorsal and lateral facet	40	44.0	48.5	12	36.5	40.2	43	9	48	55
Tn7	Depth of the distal dorsal facet	30.5	35.7	39	12	31	34.0	38	9	41	45
Tn8	Depth of the distal plantar facet	11.5	12.8	15	12	12	13.2	14.5	9	15	16
Tn9	Breadth of the distal dorsal facet	17.5	19.7	22.5	12	16	18.1	20	8	24	26

Ectomesocuneiforme		*C. bactrianus* Min	Average	Max	N	*C. dromedarius* Min	Average	Max	N	TER1680 (dex)
Tl1	Maximal breadth	31.5	35.7	38.5	12	31.5	33.8	36	8	39
Tl2	Proximal breadth	17.5	19.3	22.5	12	17	18.0	20.5	8	27
Tl3	Proximal depth	24	34.5	39	12	31	33.8	38	9	38
Tl4	Diameter of the plantar lateral facet	8	11.2	14.25	11	8	10.6	13	8	10
Tl5	Diameter of the dorsal lateral facet	16	17.4	19.75	12	12	14.5	18	8	19
Tl6	Lateral depth	27	30.4	34	11	23.5	28.3	30	8	32
Tl7	Lateral height	17	20.3	23	12	18	19.8	23	8	21
Tl8	Breadth of distal facet	20.75	23.4	26	12	18	21.1	24	8	27
Tl9	Depth of distal facet	28.5	31.9	35.5	12	28.25	30.4	35.5	9	36